Rapid response of head direction cells to reorienting visual cues: A computational model

T. Degris*, N. Brunel†, A. Arleo‡

Abstract

We model head direction (HD) cells in the rat's limbic system. The intrinsic dynamics of the HD model is determined by a continuous attractor network based on spiking formal neurons. Synaptic excitation is mediated by NMDA and AMPA formal receptors, whereas inhibition is mediated by GABA receptors. We focus on the temporal aspects of state transitions of the HD system following reorienting visual stimuli and reproduce the short transient latencies (about 80 ms) observed in the anterodorsal thalamic nucleus (ADN). A contribution of the model is an experimentally testable prediction concerning the state update dynamics as a function of the magnitude of reorientation. The results predict a progressive shift of the preferred directions of ADN cells for angles smaller than $60°$, whereas an abrupt jump is predicted for larger offsets.

1 Introduction

Head direction (HD) cells constitute a likely neural basis for the spatial orientation capabilities of rats. The response of these limbic neurons is tuned to the animal's allocentric heading in the azimuthal plane. A HD cell i discharges selectively only when the head of the animal is oriented in the preferred direction of the cell θ_i, regardless of the animal's ongoing behavior and spatial location [13, 12]. Each HD neuron i has a unique preferred direction θ_i. HD cells have been observed in a network spanning a variety of structures centered on the brain's limbic system, including postsubiculum (PSC), anterodorsal thalamic nucleus (ADN), and lateral mammillary nucleus (LMN) [12].

The preferred directions of all HD cells, $\Theta = \{ \theta_i \mid \forall i \}$, are evenly distributed over $360°$, such that the HD cell system could work as an allocentric neural compass. When the head of the animal remains oriented in a given direction θ, the subpopulation of HD cells with preferred directions $\theta_i \simeq \theta$ remains active for an indefinite period of time (demonstrating persistence of the neural coding). During head turns, the active subpopulation of HD cells provides an ongoing neural trace of the orientation of the animal $\theta(t)$, according to the head angular velocity $\omega(t)$. Inertial self-motion signals (e.g., vestibular) are likely to converge onto the HD system via subcortical projections from the dorsal tegmental nucleus (DTN) [2]. DTN receives vestibular inputs from the medial vestibular nuclei and conveys this information to LMN and ADN.

Although the HD cell system has properties resembling those of a compass, the allocentric coding of HD cells is independent of geomagnetic fields. Rather, the preferred directions are anchored to visual fixes in the environment: in a neutral setting, rotating a dominant visual cue by an angle $\Delta\theta$ induces a shift in all preferred directions such that $\Theta' = \{ \simeq \theta_i + \Delta\theta \mid \forall i \}$ [12, 17]. Based on anatomical connectivity, visual inputs are likely to enter the HD system via the postsubicular cortex and the retrosplenial cortex (which also contains HD cells [12]). The PSC receives afferents from the visual areas 17 and 18, whereas the retrosplenial cortex receives inputs from higher associative areas as the posterior parietal cortex [12].

The interrelation between idiothetic (e.g., vestibular) and allothetic (e.g., visual) cues for determining the dynamics of the HD cell system is a relevant issue for both experimental and theoretical neuroscience (e.g., [10, 1]). Recent electrophysiological studies by Zugaro et al. [16] have focused on the temporal aspects of the preferred direction updates in ADN following a $90°$ reorienting visual cue. The quantitative results show rather short update latency of approximately $80 \pm 10\ ms$.

Theoretical studies, based upon continuous attractor networks, model the ensemble activity of HD cells as a gaussian-shaped profile encoding the current head direction (e.g., [15, 11, 9]). Earlier models predicted update latencies of about $200 - 250\ ms$ for the activity profile to be reoriented by a visual cue [15, 11]. This, however, is larger than the reaction time observed experimentally. These models employed rate coding computational units, which are intrinsically limited for quantitatively describing the temporal properties of real neurons. Here, we propose a continuous attractor network model based upon spiking neurons, which permit detection of the fast update transient exhibited by HD cells in ADN.

* AnimatLab-LIP6, 8 rue du Capitaine Scott, 75015 Paris

† Lab. of Neurophysics and Physiology of the Motor System, CNRS-University Paris 5, 45 rue des Saints Peres 75270 Paris

‡ Corresponding author, Lab. de Physiologie de la Perception et de l'Action, CNRS-Collège de France, 11 pl. M. Berthelot, 75005 Paris, email: angelo.arleo@college-de-france.fr, phone: +33 (0)1 44.27.13.91, fax: +33 (0) 1 44.27.13.82

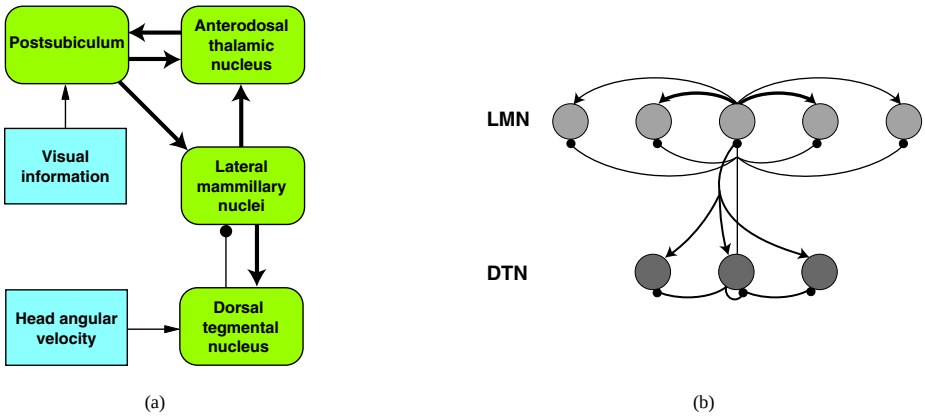

(a) (b)

Figure 1: (a) The model of the HD cell circuit (adapted from [8]). Arrows and circles indicate excitatory and inhibitory connections, respectively. An attractor-integrator network is formed by the interaction between the lateral mammillary nuclei (LMN) and the dorsal tegmental nucleus (DTN). (b) The LMN-DTN attractor module (for sake of clarity the integrator component is omitted) consists of one pool of N_E excitatory units and one of N_I inhibitory units. In the model, synaptic excitation is mediated by NMDA and AMPA receptors, whereas inhibition is mediated by GABA receptors.

2 Methods

2.1 *Global model architecture*

Fig. 1(a) shows the global architecture of the model inspired by the HD circuit of rats [8]. It includes four neural networks modeling PSC, ADN, LMN, and DTN. The dynamics of the entire system is primarily determined by idiothetic signals (e.g., vestibular) that enter the circuit via DTN and are integrated over time through the DTN-LMN interaction. This permits head rotations to be tracked based on the head angular velocity signal ω. Visual stimuli are signaled in the PSC and allow the system to reorient the directional representation following changes in the visual scene. Extrinsic background noise arrives at all formal neurons modeling external spontaneous activity. This noise is defined by a Poisson distribution.

In the model, PSC, ADN, and LMN networks consist of a population of $N_E = 1000$ excitatory directional units with evenly distributed preferred directions. The intermodule connectivity (see Fig. 1(a) for reciprocal projections) is such that, for instance, a HD unit $j \in PSC$ with preferred direction θ_j projects to a cell $i \in LMN$ with preferred direction θ_i according to

$$w_{ij} = W^- + (W^+ - W^-) \cdot \exp\Big(- \frac{(\theta_i - \theta_j)^2}{2\sigma^2} \Big) \tag{1}$$

where w_{ij} is the connection weight, W^- and W^+ are, respectively, the minimum and maximum weight, and σ is the width of the gaussian.

Similar to Blair et al. [3], we propose a continuous attractor-integrator network based on the known anatomical interconnections between LMN and DTN (Fig. 1(b)). The HD cells within LMN are connected by recurrent excitatory collaterals such that neurons encoding similar states (i.e., having similar preferred directions) are strongly coupled. The weight of the collateral projection between cells $i, j \in LMN$ is defined according to Eq. 1. Global inhibition, necessary to implement the center-surround attractor scheme, is provided by a population of interneurons $\xi \in DTN$. Each ξ cell receives excitatory afferents from all LMN cells, and inhibits all LMN directional neurons as well as all ξ interneurons. The intrinsic dynamics of the LMN-DTN$_\xi$ attractor network make the system settle down to stable (self-sustained) attractor states, in which subpopulations of HD cells with similar preferred directions are active while the others remain silent [15, 3]. In other words, for zero angular velocity $\omega = 0$, the ensemble activity profile of HD cells will persistently code for a direction θ.

To integrate non-zero angular velocities (i.e., to shift the stable state over the continuous attractor state space according to ω), two other subpopulations of interneurons $\xi_{cw}, \xi_{ccw} \in DTN$ are considered [3]. The neuronal responses of the ξ_{cw}, ξ_{ccw} cells are correlated with both head direction $\theta(t)$ and angular velocity $\omega(t)$. An interneuron $j \in \xi_{cw}$ with preferred direction θ_j receives excitatory afferents from all HD cells $i \in LMN$. The weights of these connections are defined by Eq. 1 (i.e., gaussian-distributed matching projections). The interneuron $j \in \xi_{cw}$ sends inhibitory efferents to all HD cells $i \in LMN$ by means of a gaussian weight distribution centered at $\theta_i = \theta_j - \delta$, with $\delta = 50°$, (i.e., gaussian-distributed leftward offset projections). Similarly, each ξ_{ccw} interneuron receives gaussian-distributed matching inputs from LMN and sends gaussian-distributed rightward offset inhibition to LMN. The activity of ξ_{cw} and ξ_{ccw} formal neurons is linearly modulated by the amplitude of the angular velocity $|\omega|$ for $\omega > 0$ and $\omega < 0$, respectively. Therefore, during clockwise head turns for instance, ξ_{cw} cells inhibit the left side of the

LMN hill of activity encoding the current direction θ (i.e., introduce an asymmetry within the recurrent coupling between HD cells [15, 3]) and yield a clockwise shift $\Delta\theta$ proportional to $|\omega|$.

At any time t, the direction representation $\theta(t)$ encoded by the LMN ensemble activity is transmitted to the other subnetworks of the system, via the LMN-ADN-PSC excitatory pathway (Fig. 1(a)).

2.2 *Neuron and synapse model*

The formal description of neurons and synapses of the model is directly inspired from Brunel and Wang [4]. Both HD cells and interneurons are leaky integrate-and-fire neurons [14]. Synaptic excitation is mediated by NMDA and AMPA formal receptors, whereas synaptic inhibition is mediated by GABA receptors. The rationale behind using two different excitatory receptors is the following: AMPA synapses are rapidly activated and generate fast evoked responses of postsynaptic neurons. However, their short time decay ($\tau_{decay} = 2\ ms$) does not permit an appropriate stabilization of the network activity. On the other hand, the larger time course of the NMDA receptors ($\tau_{decay} = 100\ ms$) is suitable for the stability issue.

2.3 *Population vector coding*

As described in Sec. 2.1, the model encodes the ongoing animal's heading by means of a gaussian-shaped activity profile distributed over all HD cells. In order to reconstruct the current head direction $\theta(t)$, we apply a population vector scheme [7] to decode the ensemble HD cell activity:

$$\theta(t) = \arctan\left(\frac{\sum_i^{N_E} sin(\theta_i)\delta(t-t_i)}{\sum_i^{N_E} cos(\theta_i)\delta(t-t_i)}\right) \quad (2)$$

where the function $\delta(t-t_i)$ is equal to 1 if the neuron i fired at time t, 0 otherwise.

3 Results

In this paper, we focus on the effect of static visual stimulation upon the intrinsic dynamics of the HD cell system. An external excitatory input $\vec{v}$ is applied to the pool of HD cells in the PSC, which propagates this information to the LMN-DTN attractor network (eventually yielding a change of the attractor state) as well as to ADN. We take $\vec{v}$ as a gaussian signal with fixed width $\sigma_v = 15°$, variable amplitude $A_v \in [0, 1]$ (corresponding to the intensity of the visual stimulation), and variable mean $\mu_v = \theta_v$ (corresponding to the absolute direction of the polarizing cue). Note that, due to the properties of the attractor network, the shape of the stimulus profile (e.g., gaussian, rectangular, and so on) does not influence the characteristics of the self-sustained activity profile (e.g., shape and width) which the system settles down to.

3.1 *Emergence and stability of an attractor state*

The rastergram of Fig. 2(a) shows the spike activity of the N_E ADN cells over time[1]. A polarizing stimulus $\vec{v}$ centered at $\theta_v = 90°$ and of normalized amplitude $A_v = 0.2$ is applied during the first $50\ ms$. This establishes a stable attractor state corresponding to an ensemble activity profile in which the subpopulation of ADN neurons having preferred directions close to θ_v discharge tonically, whereas the others exhibit a very low baseline frequency. Since an attractor state would eventually emerge from random noise, a stimulus of weak intensity A_v is sufficient to polarize the system around θ_v. The center of mass of the ensemble firing pattern, computed by applying Eq. 2 and averaging over $\Delta t = 2\ s$, is about $\overline{\theta} = 85°$. Fig. 2(b) shows the mean firing rate $\overline{r}_i$ of all HD cells i in ADN. The mean spike frequency $\overline{r}_i$ is computed by averaging over the time window $\Delta t = 2\ s$. The mean peak firing rate is about $40\ spikes/s$ whereas the width of the hill of activity is about $100°$. These values are consistent with the mean peak firing rate and the mean width of the tuning curves of real HD cells in ADN [12].

After stimulus removal (e.g., moving from light to dark conditions) the self-sustained attractor state persists over time ($50 \leq t \leq 2000\ ms$ in Fig. 2(a)) providing a stable directional coding (the head angular velocity ω is zero). This corresponds to the situation in which the head of the animal is immobile and oriented in a given direction θ_v and all real HD cells with $\theta_i \simeq \theta_v$ continue to discharge tonically.

3.2 *Short update latencies following reorienting visual stimuli*

Fig. 3(a) shows the response of the system to a reorienting visual stimulus. At time $t_1 = 500\ ms$, an external stimulus $\vec{v}_1$ is applied to the system (e.g., moving from dark to light conditions) with a $90°$ offset, i.e. $\mu_{v_1} = \theta_v + 90°$. This triggers a $90°$ update of all preferred directions, which reorients the HD system according to the directional reference frame anchored to $\vec{v}_1$. As a consequence, the attractor network settles to a new stable state abruptly. The intensity of the applied stimulus is $A_{v_1} = 1$. For a $90°$ offset, in our simulations, only those stimuli with $A_v \geq 0.6$ were able to trigger a change of attractor state.

[1] All results have been obtained by means of computer simulations employing a RK2 numerical integration of the equations describing the dynamics of formal neurons and synapses. The integration step was $dt = 1\ ms$.

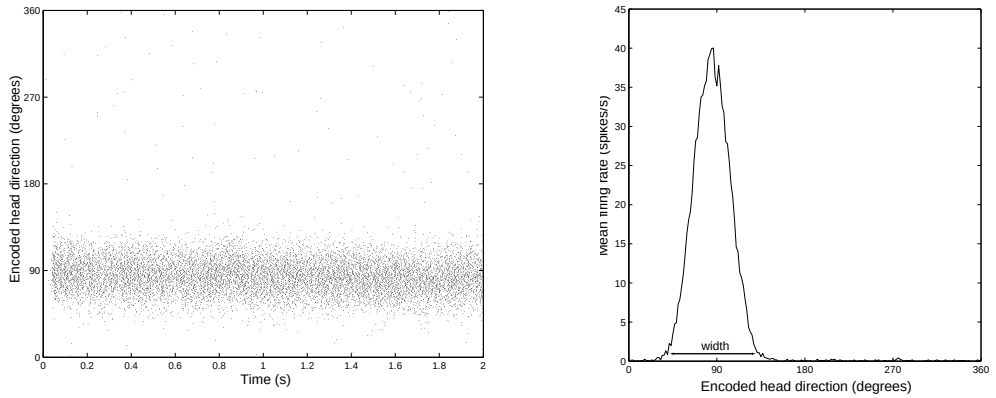

(a) (b)

Figure 2: (a) Rastergram of the activity of the HD cells in ADN over time (each dot represents a spike). A polarizing external stimulus (applied at $90°$ during the first $50\ ms$) establishes a stable attractor state. After stimulus removal ($t \geq 50\ ms$) the self-sustained state persists over time. (b) Mean firing rate of all ADN cells computed by averaging over $\Delta t = 2\ s$. The mean peak firing rate is about $40\ spikes/s$ whereas the width of the hill of activity is about $100°$.

Let Δt_* be the transient latency quantifying the time necessary for the attractor dynamics to update its state. To measure Δt_* we apply the same technique employed by Zugaro et al. [16] to quantify the update response of HD cells in ADN. First, we build the spike peri-event histogram for the subpopulation of HD cells that become active after the stimulus onset, $t \geq t_1$, (Fig. 3(b)). We take a $10\ ms$ bin and focus on the time interval $t_1 - 500 \leq t \leq t_1 + 500\ ms$. Second, we build the corresponding cumulative histogram and determine the transition point t_* between the best fit slopes based on the least square error method (Fig. 3(c)). The resulting update latency is $\Delta t_* = t_* - t_1 = 40 \pm 10\ ms$, which estimates the time necessary for the new subpopulation of HD cells to become fully activated. This result is consistent with the update latency reported by Zugaro et al. [16], i.e. $\Delta t_* = 80 \pm 10\ ms$. Note that our model does not take into account the transmission delay necessary for the visual signals to reach HD cells in ADN. We are not aware of any experimental data reporting this retino-thalamic transmission time, however Galambos et al. [6] showed that about $30\ ms$ are already necessary for the visual stimulation of the retina to evoke field potentials in the primary visual cortex.

3.3 *Studying the state transition dynamics: Abrupt jump or progressive shift?*

Whether real HD cells respond to visual reorientation by changing their preferred directions abruptly or in a gradual progressive manner, is an open question [12, 16]. Note that, the 'abrupt *versus* progressive update' issue is also relevant for the theoretical study of state transition dynamics in associative memories [5].

As shown in Fig. 3, our simulations suggest that an abrupt jump occurs when a salient $90°$ reorienting visual cue polarizes the HD system. We now ask the question: For a fixed width of the gaussian-shaped activity profile, how does the magnitude of the reorienting offset $\Delta\theta$ influence the state transition dynamics of the system? We run a series of simulations in which the same external stimulus $\vec{v}_1$ ($A_{v_1} = 1$) is applied to the HD system at time $t_1 = 500\ ms$. Across trials, the reorienting offset $\Delta\theta = \mu_{v_1} - \theta_v$ (with $\theta_v = 90°$) is varied within $[0°, 180°]$ by steps of $1°$.

Fig. 4(a) shows an example of state transition for $\Delta\theta = 40°$. The HD cells respond to the reorienting event by progressively shifting their preferred directions towards the new attractor state. To discriminate between state transitions of the type shown in Fig. 3(a) (jump) and those of the type in Fig. 4(a) (shift), we take the instantaneous standard deviation $\sigma(t)$

$$\sigma(t) = \Big(\frac{\sum_i^{N_E} [|\theta_i - \theta(t)| \cdot \delta(t - t_i)]^2}{\sum_i^{N_E} \delta(t - t_i)} \Big)^{\frac{1}{2}} \tag{3}$$

of the ensemble HD cell activity around the center of mass $\theta(t)$ (Eq. 2)[2]. Fig. 4(b) shows the standard deviation $\sigma(t)$ over time in the case of $\Delta\theta = 90°$ (corresponding to the transition of Fig. 3(a)) and in the case of $\Delta\theta = 40°$ (corresponding to the transition of Fig. 4(a)). We sample all $\sigma(t)$ values within the interval $t_1 \leq t \leq t_1 + 200\ ms$ and take the mean deviation $\overline{h}$ relative to the baseline. Fig. 4(c) shows $\overline{h}$ as a function of all tested offsets $\Delta\theta \in [0°, 180°]$. Let $\Delta\theta_*$ be the critical offset above which the reorienting visual cue triggers a jump rather than a progressive shift. As expected, the function $\overline{h}(\Delta\theta)$ is approximately constant

[2]Note that in Eq. 3 the actual implementation of the deviation $d_i(t) = |\theta_i - \theta(t)|$ is

$$d_i(t) = \begin{cases} \min(|\,\theta_i - \theta(t)\,|,\ |\,\theta(t) - \theta_i + 360\,|) & \theta_i > \theta(t) \\ \min(|\,\theta_i - \theta(t)\,|,\ |\,\theta_i - \theta(t) + 360\,|) & otherwise \end{cases} \tag{4}$$

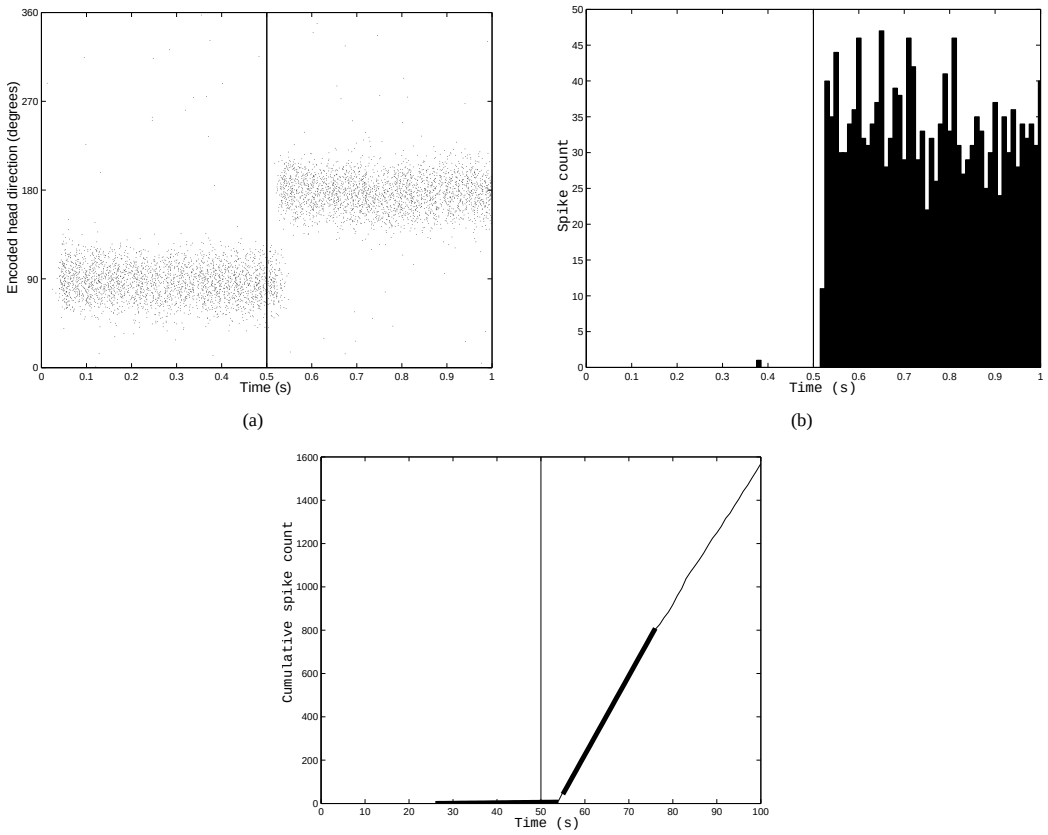

Figure 3: (a) Raster plot showing the response of the HD system to a $90°$ reorienting visual stimulus applied at time $t_1 = 500\ ms$. All preferred directions are updated and the attractor network settles to a new stable state abruptly (jump). (b) Spike peri-event histogram ($10\ ms$ bin) for the subpopulation of HD cells that become active after the stimulus onset, $t \geq 500\ ms$. (c) Cumulative histogram (thin line). To determine the transition point between the best fi t slopes, the least square error is computed (thick line). The resulting update latency is $40 \pm 10\ ms$.

for $0 \leq \Delta\theta \leq \Delta\theta_*$ and quasi-linear after. Our results show that $\Delta\theta_*$ (computed by applying the least square error method) is equal to $60 \pm 5°$.

4 Discussion

This paper describes a computational model of the rat's head direction (HD) system. In contrast to earlier works (e.g., [15, 11, 9]) that use rate code formal neurons to model HD cells, we employ spiking neurons and focus on the temporal aspects of state transition dynamics following reorienting visual stimulation.

Recent experimental findings by Zugaro et al. [16] suggest that HD cells in ADN are capable to update their directional response as rapidly as $80 \pm 10\ ms$ after changes in the visual scene ($90°$ cue card rotations). The first contribution of our model, which has a modular neural architecture based on the anatomical circuitry of the HD system, is that it can reproduce these short transient latencies observed in ADN. In the model, formal ADN neurons respond as rapidly as $40\ ms$ to a $90°$ reorienting visual cue. The shorter update latencies of the simulated HD cells are due to the fact that the model does not account for retino-thalamic transmission delays.

The second contribution of this work is an experimentally testable prediction concerning the state transition dynamics of the HD system as a function of the magnitude of the angle of rotation (directional offset $\Delta\theta$). The results suggest that a salient visual stimulus will yield a progressive shift of the preferred directions of ADN cells for $\Delta\theta \leq 60°$, whereas an abrupt jump will occur for larger offsets.

Acknowledgments

This work was supported by the ACI du Ministère de la Recherche and the ROBEA program of the CNRS. The authors thank S. I. Wiener, M. B. Zugaro, and C. C. Boucheny for useful discussions.

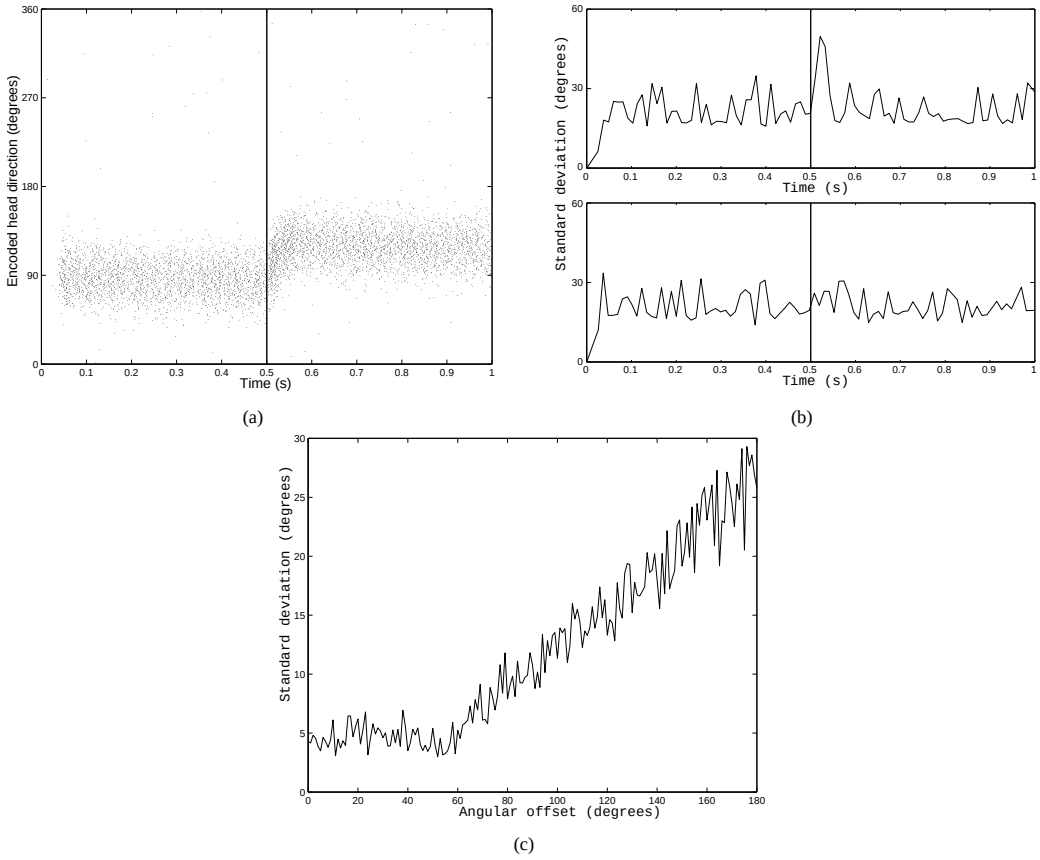

Figure 4: (a) Response of the HD system to a $40°$ reorienting stimulus applied at time $t_1 = 500\ ms$. The HD cells shift their preferred directions towards the new attractor state progressively. (b) Standard deviation $\sigma(t)$ around the center of mass of the activity blob. Above: in the case of a $90°$ update. Below: in the case of a $40°$ update. (c) Mean deviation of $\sigma(t)$ (within the interval $t_1 \leq t \leq t_1 + 200\ ms$) relative to its baseline as a function of the reorienting rotation angle (offset). The transition point (computed by the least square error method) is at about $60 \pm 5°$.

References

[1] A. Arleo and W. Gerstner. *Neurocomputing*, 38-40(1-4):1059–1065, 2001.
[2] J. P. Bassett and J. S. Taube. *J. Neuroscience*, 21(15):5740–5751, 2001.
[3] H. T. Blair, J. Cho, and P. E. Sharp. *Neuron*, 21:1387–1397, 1998.
[4] N. Brunel and X.-J. Wang. *J. Comp. Neuroscience*, 11:63–85, 2001.
[5] J. Droulez and A. Berthoz. In *Proc. Natl. Acad. Sci. USA*, volume 88, pages 9653–9657, USA, 1991.
[6] R. Galambos, O. Szabo-Salfay, P. Barabas, J. Palhalmi, N. Szilagyi, and G. Juhasz. *Proc. Natl. Acad. Sci. USA*, 97(24):13454–13459, 2000.
[7] A. P. Georgopoulos, A. Schwartz, and R. E. Kettner. *Science*, 233:1416–1419, 1986.
[8] J. P. Goodridge and J. S. Taube. *J. Neuroscience*, 17(23):9315–9330, 1997.
[9] J. P. Goodridge and D. S. Touretzky. *J. Neurophysiology*, 83(6):3402–3410, 2000.
[10] J. J. Knierim, H. S. Kudrimoti, and B. L. McNaughton. *J. Neurophysiology*, 80:425–446, 1998.
[11] A. D. Redish, A. N. Elga, and D. S. Touretzky. *Network*, 7(4):671–685, 1996.
[12] J. S. Taube. *Progress in Neurobiology*, 55:225–256, 1998.
[13] J. S. Taube, R. I. Muller, and J. B. Ranck Jr. *J. Neuroscience*, 10:420–435, 1990.
[14] H. C. Tuckwell. *Introduction to Theoretical Neurobiology*. Cambridge University Press, Cambridge, 1996.
[15] K. Zhang. *J. Neuroscience*, 16(6):2112–2126, 1996.
[16] M. B. Zugaro, A. Arleo, A. Berthoz, and S. I. Wiener. *J. Neuroscience (in press)*, 2003.
[17] M. B. Zugaro, A. Berthoz, and S. I. Wiener. *J. Neuroscience*, 21(RC154):1–5, 2001.